EPSC Abstracts
Vol. 5, EPSC2010-360, 2010
European Planetary Science Congress 2010

Correlations between VIMS and RADAR data over the surface of Titan: Implications for Titan's surface properties

F. Tosi (1), R. Orosei (1), R. Seu (2), A. Coradini (1), J.I. Lunine (3), G. Filacchione (4), F. Capaccioni (4), P. Cerroni (4), R.H. Brown (5), and the Cassini VIMS and RADAR Teams

(1) INAF-IFSI, Via del Fosso del Cavaliere 100, I-00133 Rome, Italy (federico.tosi@ifsi-roma.inaf.it / Fax: +39-06-49934702), (2) Università di Roma “La Sapienza”, Dipartimento INFOCOM, Via Eudossiana 18, I-00184 Rome, Italy, (3) Università degli Studi di Roma "Tor Vergata", Dipartimento di Fisica, Via della Ricerca Scientifica 1, I-00133, Rome, Italy, (4) INAF-IASF, Via del Fosso del Cavaliere 100, I-00133, Rome, Italy, (5) Lunar and Planetary Lab, University of Arizona, 1629 E. University Blvd., Tucson, AZ 85721-00092, USA.

Abstract

We apply a multivariate statistical method to Titan data acquired by different instruments onboard the Cassini spacecraft. We have searched through Cassini/VIMS [1] hyperspectral cubes, selecting those data with convenient viewing geometry and that overlap with Cassini/RADAR [2] scatterometry footprints with a comparable spatial resolution. We look for correlations between the infrared and microwave ranges the two instruments cover. Where found, the normalized backscatter cross-section obtained from the scatterometer measurement, corrected for incidence angle, and the calibrated antenna temperature measured along with the scatterometry echoes, are combined with the infrared reflectances, with estimated errors, to produce an aggregate data set, that we process using a multivariate classification method to identify homogeneous taxonomic units in the multivariate space of the samples.

1. Introduction

We present new results combining the VIMS and RADAR data on Titan’s surface. In RADAR data we consider two geophysical quantities: the normalized backscatter cross-section obtained from the scatterometer measurement, corrected for the incidence angle, and the calibrated antenna temperature determined from the radiometer measurement, as found in publicly available data products. In VIMS data, combining spatial and spectral information, we have selected some atmospheric windows in the spectral range between 2 and 5 μm, providing the best optical depth to measure surface reflectance.

The two RADAR parameters are combined with VIMS data, with estimated errors, to produce an aggregate data set, that we process using a multivariate classification method to identify homogeneous taxonomic units in the multivariate space of the samples. The use of data sets from different instruments onboard the Cassini spacecraft has the potential to deepen our understanding of the nature of the surface.

Our analysis relies on the *G-mode* [3], an unsupervised clustering method that has been successfully used in the past for the classification of such diverse data sets as lunar rock samples, asteroids and planetary surfaces. Due to the large number of data of Titan, the classification work proceeds in several steps. In a previous work [4], we analyzed the data acquired in Titan flybys: T3, T4, T8, T13 and T16, covering mostly the major bright and dark features seen around the equator, combined with VIMS infrared data, in order to validate the classification method. Now we focus on flybys: T23, T25, T28, T30, and T43, covering also regions of Titan located at higher latitudes.

2. Results

The obtained results are generally in agreement with previous work devoted both to the analysis of the scatterometry data through physical models and to the correlation between SAR and radiometry data at a high resolution scale.

In general, dark basins like Belet and Senkyo behave the same way as other dark equatorial basins already explored in our previous analysis [4], appearing dark in all of the atmospheric windows between 2 and 5 μm and showing at the same time a low backscattering coefficient and a higher antenna temperature (when it is considered), the first parameter being indicative of a small roughness and/or composition [5] while the latter parameter is also consistent with the higher emissivity of the material these regions are filled of [6]. On the other hand, optically bright features show a variety of behaviors at different spatial scales: on a regional scale they appear bright also in the methane windows from 2 to 5 µm, but not necessarily at the same degree and with possible differences related also to the backscattering coefficient. This evidence is likely related to surface composition (e.g., different concentrations of simple ices and/or hydrocarbons), and it becomes even more detailed by increasing the spatial resolution of the data, with small homogeneous types showing subtle differences in some of the explored variables. Furthermore, volume scattering effects can also play a role, and are revealed by diagnostic combination of the backscattering coefficient and antenna temperature values.

3. Figures

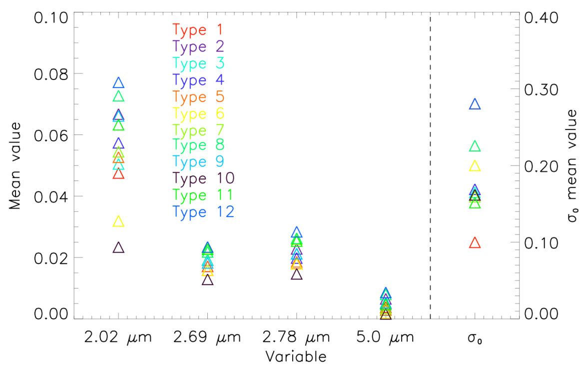

Figure 1. Classification of cube CM_155908941_1 with 5 variables. Mean values of the variables for the 12 types identified by the G-mode analysis.

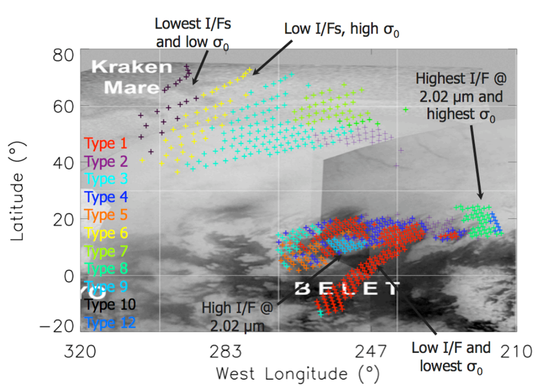

Figure 2. Classification of cube CM_155908941_1 with 5 variables. Spatial distribution of the samples superimposed to an ISS optical mosaic [7].

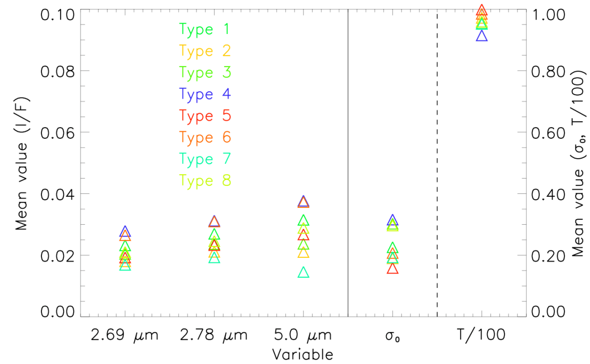

Figure 3. Classification of cube CM_1627151462_1 with 5 variables (including the antenna temperature). Mean values of the variables for the 8 types identified by the G-mode analysis.

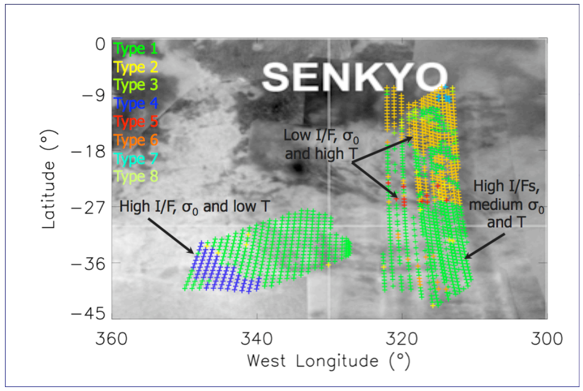

Figure 4. Classification of cube CM_1627151462_1 with 5 variables (including antenna temperature). Spatial distribution of the samples superimposed to an ISS optical mosaic [7].

Acknowledgements

This work was supported by the Italian Space Agency, ASI-INAF grants I/031/05/0 and I/026/05/0.

References

[1] Brown, R.H. et al. (2004) *Space Sci. Rev. 115*, Issue 1-4, 111-168.
[2] Elachi, C. et al. (2004) *Space Sci. Rev. 115*, Issue 1-4, 71-110.
[3] Coradini, A. et al. (1977) *Comput. Geosci. 3*, 85-105.
[4] Tosi, F., et al. (2010) *Icarus*, in press.
[5] Wye, L.C. et al. (2007), *Icarus 188*, 367-385.
[6] Janssen, M.A., et al. (2009) *Icarus* 200, 222-239.
[7] Turtle, E., et al. (2009), *Geophys. Res. Lett.* 36, L02204.